*Technical Physics, Vol. 50, No. 4, 2005, pp. 385–393. Translated from Zhurnal Tekhnicheskoĭ Fiziki, Vol. 75, No. 4, 2005, pp. 1–10.*
*Original Russian Text Copyright © 2005 by Koronovskii, Popov, Khramov.*

**THEORETICAL AND MATHEMATICAL PHYSICS**

# Chaotic Synchronization of Unidirectionally Coupled Electron-Wave Media with Interacting Counterpropagating Waves

**A. A. Koronovskii, P. V. Popov, and A. E. Hramov**

*Chernyshevsky State University, Kolledzh State Educational and Scientific Center, Saratov, 410026 Russia*
*e-mail: alkor@cas.ssu.runnet.ru, aeh@cas.ssu.runnet.ru*

Received April 26, 2004

**Abstract**—Chaotic synchronization of two electron-wave media with interacting counterpropagating waves and cubic phase nonlinearity (transverse-field backward-wave oscillators) is studied. Analysis is based on considering a continuous set of the phases of a chaotic signal. The parameters of chaotic synchronization in a system of unidirectionally coupled backward-wave oscillators are found, and the complex dynamics of establishing the chaotic synchronization conditions in an active medium is investigated. © *2005 Pleiades Publishing, Inc.*

## INTRODUCTION

Investigation into chaotic synchronization of self-oscillations is a prominent problem in the modern theory of nonlinear oscillations and waves [1, 2]. This phenomenon is observed in a variety of systems, including physical and biological systems [3–6]. Investigation of this phenomenon is of great importance as applied to data transmission by means of determinate chaotic oscillations [7]. In most cases, chaotic synchronization was studied in systems with a small number of degrees of freedom. In distributed electron-wave systems, such investigations have not been carried out, although this problem seems central to microwave electronics (see, e.g., [8–10]).

Different types of chaotic synchronization are distinguished: phase synchronization, generalized synchronization, lag, and complete synchronization [2]. Phase synchronization, which is described through the phase $\phi(t)$ of a chaotic signal [11, 12], means that the phases of chaotic signals lock in synchronism, while their amplitudes remain unrelated to each other and appear chaotic. Phase lock-in results in coincidence of the frequencies of the signals. The frequency of a chaotic signal is defined as the mean rate of change of phase $\phi(t)$. However, it does not always happen that the system can be characterized by a single phase especially if the signal has a complex spectral composition [13].

In [14], we suggested a new approach to analysis of chaotic synchronization that is based on considering a continuous set of phases. This set is determined by the continuous wavelet transform [15, 16] of chaotic signal $x(t)$,

$$W(s, t_0) = \int_{-\infty}^{+\infty} x(t)\psi^*_{s, t_0}(t)dt, \quad (1)$$

where $\psi_{s, t_0}(t)$ is a wavelet function derived from generating wavelet $\psi_0(t)$,

$$\psi_{s, t_0}(t) = \frac{1}{\sqrt{s}}\psi_0\left(\frac{t - t_0}{s}\right). \quad (2)$$

Time scale $s$ specifies the width of wavelet $\psi_{s, t_0}(t)$; $t_0$, the shift of the wavelet function along the time axis (the asterisk in (1) means the complex conjugate) [16]. Note that, in wavelet analysis, the notion "time scale" is routinely used instead of the notion "frequency," which is generally accepted in conventional Fourier transformation.

As a generating wavelet, we apply Morlet wavelet $\psi_0(\eta) = (1/\sqrt[4]{\pi})\exp(j\omega_0\eta)\exp(-\eta^2/2)$ [16]. Setting wavelet parameter $\omega_0$ equal to $2\pi$ ($\omega_0 = 2\pi$), provides the relationship $s = 1/f$, where $s$ is the time scale of wavelet transformation and $f$ is the frequency of Fourier transformation.

Wavelet spectrum

$$W(s, t_0) = |W(s, t_0)|\exp[j\phi_s(t_0)] \quad (3)$$

describes the behavior of the system on each time scale $s$ at any time $t_0$. The value of $|W(s, t_0)|$ characterizes the presence and significance of corresponding time scale $s$ at time $t_0$. It is convenient to introduce the integral dis-

1063-7842/05/5004-0385$26.00 © 2005 Pleiades Publishing, Inc.

tribution of the wavelet energy over the time scales,

$$\langle E(s)\rangle = \int |W(s, t_0)|^2 dt_0. \quad (4)$$

Concurrently, phase $\psi_s(t) = \arg W(s, t)$ becomes definite in a natural way for each of time scales $s$. In other words, it becomes possible to characterize the behavior of each of time scales $s$ through its associated phase $\psi_s(t)$.

If there exists time scale interval $[s_1, s_2]$ such that the condition of phase lock-in

$$|\psi_{s1}(t) - \psi_{s2}(t)| < \text{const} \quad (5)$$

is met for any time scale $s \in [s_1, s_2]$ and if part of the wavelet spectrum energy falling into this interval is other than zero,

$$E_{\text{sync}} = \int_{s_1}^{s_2} \langle E(s)\rangle ds > 0, \quad (6)$$

time scales $s \in [s_1, s_2]$ are synchronized and the chaotic oscillators are under the condition of time scale synchronization [14]. In (5), $\psi_{s1,2}(t)$, the continuous phases of the first and second oscillators, correspond to synchronized time scales $s$.

In this work, the above approach is applied to studying chaotic synchronization in a model system of coupled electron-wave media with counterpropagating waves and cubic phase nonlinearity (coupled transverse-field backward-wave oscillators, BWOs). This is the simplest model of microwave oscillators based on backward-wave tubes, which are of considerable current use [17].

## 1. MODEL UNDER INVESTIGATION

Consider the basic equations that describe our model of two coupled electron-wave media with counterpropagating waves and cubic phase nonlinearity.

In a linear approximation, interaction between two counterpropagating dispersionless waves van be described by the set of equations

$$\frac{\partial F}{\partial \tau} - \frac{\partial F}{\partial \xi} = -AI, \quad (7)$$

$$\frac{\partial I}{\partial \tau} + \frac{\partial I}{\partial \xi} = -AF, \quad (8)$$

where $F = |F|\exp[j\varphi_F]$ and $I = |I|\exp[j\varphi_I]$ are the amplitudes of the electromagnetic and electron waves, respectively, which slowly (compared with $\exp(j(\hat{\omega}t - \hat{k}\xi))$ vary in time and space; $\tau$ and $\xi$ are the dimensionless time and coordinate, respectively; $\hat{\omega}$ and $\hat{k}$ are, respectively, the frequency and wavenumber that correspond to the point of interaction between the dispersion curves for noninteracting electron and electromagnetic waves; and $A$ is a dimensionless control parameter, which can be considered as the dimensionless length of the system or the dimensionless current of the electron beam [18].

A solution to linear equations (7) and (8) predicts the exponential growth of the amplitude of either wave. For oscillations in the system of the interacting waves to become stable, any nonlinear effect in the electron wave should be taken into account. A simple nonlinear effect is nonisochronism of electronic oscillators, which shows up in the dependence of the frequency of an electronic oscillator on its energy [17, 19]. Nonisochronism of electronic oscillators in our system of interacting counterpropagating waves is embodied in the nonlinear variation of phase $\varphi_1$ of the electron wave.

Let us assume that the part of phase $\varphi_1$ of the electron wave that is proportional to longitudinal coordinate $\xi$ linearly depends on wave energy $W = \alpha I^2$ ($\alpha$ is a proportionality coefficient) in a first approximation. Then, the radiation frequency shifts because of the Doppler effect [19]. In the coordinate system with shifted time, $\tau' = (\tau - \xi)/2$ and $\xi' = \xi$, Eq. (8) can be recast in the form

$$\frac{\partial I}{\partial \xi} + j|I|^2 I = -AF, \quad (9)$$

where the primes at the new variables are omitted.

The set of Eqs. (7) and (9) describes processes occurring in the system of interacting counterpropagating waves with cubic phase nonlinearity (BWOs). In the regime of self-induced oscillation, Eqs. (7) and (9) should be complemented by standard boundary conditions $F(\xi = 1, \tau) = 0$ and $I(\xi = 0, \tau) = 0$, which reflect the absence of both waves at the system's boundaries. The autonomous nonlinear dynamics of transverse-field BWOs in the case of increasing bifurcation parameter $A$ has been considered in detail elsewhere [18, 20, 21]. At $\pi/2 < A < 1.83$, one-frequency oscillations with stationary spatial distributions $F(\xi)$ and $I(\xi)$ set up in the system. For $A > 1.83$, the system generates multiple-frequency periodic oscillations (field periodic self-modulation). Note that, when $A > 2.05$, the pattern of input field $F(\tau, \xi = 0)$ consists of pulses with ripple in between. The ripple appears as a result of complex multiple-hump distributions $F(\xi)$ and $I(\xi)$ occurring in the system. Such distributions arise because of a fast nonlinear variation of the electron wave phase along the coordinate of the pace of interaction. Finally, at $A > 4.1$, chaotic self-oscillations are excited [21].

We will consider a system of two unidirectionally coupled electron-wave media exhibiting chaotic dynamics. The system is described by the set of equations

$$\frac{\partial F_{1,2}}{\partial \tau} - \frac{\partial F_{1,2}}{\partial \xi} = -A_{1,2} I_{1,2}, \quad (10)$$

$$\frac{\partial I_{1,2}}{\partial \xi} + j|I_{1,2}|^2 I_{1,2} = -A_{1,2}F_{1,2}, \quad (11)$$

where subscripts 1 and 2 refer to the "master" and "slave" active media, respectively.

Unidirectional coupling between the self-oscillating media is taken into account through a nonstationary boundary condition for the slowly varying amplitude of field $F_2$ of the slave active medium. In so doing, the boundary condition for the master medium remains unchanged,

$$I_1(\xi = 0, \tau) = 0, \quad F_1(\xi = 1.0, \tau) = 0, \quad (12)$$

$$I_2(\xi = 0, \tau) = 0,$$
$$F_2(\xi = 1.0, \tau) = \rho F_1(\xi = 0.0, \tau), \quad (13)$$

where $\rho = R\exp[j\theta]$ is the complex coupling coefficient ($R$ and $\theta$ are its amplitude and phase, respectively).

Note that coupling thus stated (a control signal acts only at the boundary of a distributed active medium) is natural and physically feasible unlike the situation where coupling was assumed to be spatially uniform, i.e., a control signal acted (was received) at any point of coupled active media (see [2, 22], where chaotic synchronization of distributed model media was considered).

The values of the control parameters were set equal to $A_1 = 4.2$ (master) and $A_2 = 4.9$ (slave), which meets the condition of field chaotic self-modulation. Phase $\theta$ of the coupling coefficient did nor influence the processes in the coupled system and was taken to be constant, $\theta = \pi$. Below, we analyze chaotic synchronization of two distributed electron-wave systems that is established under the condition of varying coupling coefficient amplitude $R$.

## 2. CHAOTIC SYNCHRONIZATION

Consider the behavior of the coupled system with the master and slave control parameters specified above in the case of increasing coupling coefficient amplitude $R$. Emphasis will be on oscillations $F_{r1,2} = \mathrm{Re}[F_{1,2}(\xi = 0, \tau)]$ at the exit from either medium.

Figure 1a and 1b show the oscillation power spectra and oscillation phase portraits (reconstructed by the Takens time-delay embedding method [23]) at the exit from the master and slave media, respectively, under the condition of self-excited oscillations ($R = 0$). From Fig. 1a, it follows that output field $F_{r1}$ of the master medium, which is applied to the input of the space of interaction of the slave medium ($\xi = 1$), exhibits the Fourier spectrum of the oscillation power, which corresponds to chaotic oscillations. Two clearly cut peaks at frequencies $f_m$ and $f_b$ (basic frequencies) are observed against the continuous background noise (at a level of roughly –30 dB) in Fig. 1a. Frequency $f_b$ is close to synchronism frequency $\omega$ of related noninteracting linear waves. As dimensionless current $A_1$ in the distributed system decreases, periodic oscillations set up at a frequency close to microwave frequency $\omega$. The other frequency, $f_m$, which lies in the low-frequency part of the spectrum, determines the characteristic frequency of low-frequency modulation of field amplitude $F_1$. With increasing bifurcation parameter $A$, the oscillation pattern in the system becomes more tangled, as is clearly seen in Fig. 1b, where the oscillation power spectrum is plotted for $A_2 = 4.9$ and $R = 0$ (self-excited oscillation). In the most part of the power spectrum, the noise pedestal is rather high (within –5…–10 dB), so that any characteristic oscillation frequencies can no longer be distinguished from the background.

Consider the behavior of the slave system when its interacts with the field of the master system as amplitude $R$ of the coupling coefficient between the distributed self-oscillating systems grows. Note that the power of the external signal acting on the slave system grows as $R_2$.

When $R$ increases, the oscillation spectrum of the slave system changes, as demonstrated in Figs. 1c and 1d. At small $R < 0.3$ (Fig. 1c), a weak peak (marked by an arrow) corresponding to frequency $f_b$ in the master spectrum (Fig. 1a) appears against the appreciable background. At large $R > 0.3$, the energy of the spectral components that correspond to the basic frequencies in the master spectrum rises in the slave spectrum (Fig. 1d, $R = 0.5$).

It should be noted that the phase portrait of the system (Fig. 1) does not allow us to correctly introduce the phase of the chaotic signal by any of the conventional methods [11–13] because of the complex pattern of the chaotic attractor. Therefore, introduction of a family of phases by means of the wavelet transformation [14] (see also [24]) seems to be the only effective way of studying the chaotic synchronization of coupled electron-wave oscillators.

Figure 2 shows boundaries $s_1$ and $s_2$ of the ranges of synchronized time scales on plane ($R$, $s$).

A feature of the dynamics of two coupled electron-wave media is that, at a relatively large value of coupling coefficient $R$, the time scales of chaotic signals from either subsystem become synchronized in the ranges near basic time scales $s_b = 1/f_b$ and $s_m = 1/f_m$, respectively. In Fig. 2, the ranges of the synchronized scales are shown near basic scales $s_b$ (lower part) and $s_m$ (upper part).

From Fig. 2, it follows that, at $R \in (0, 0.029)$, chaotic synchronization is not established. This means that there is no time scales $s$ where the phase dynamics meets chaotic synchronization condition (5). As coupling coefficient amplitude $R$ increases, scale range $\Delta s = s_2 - s_1$ appears where phase lock-in condition (5) is met and the energy corresponding to this range (see (6)) is other than zero. Accordingly, the regime of time

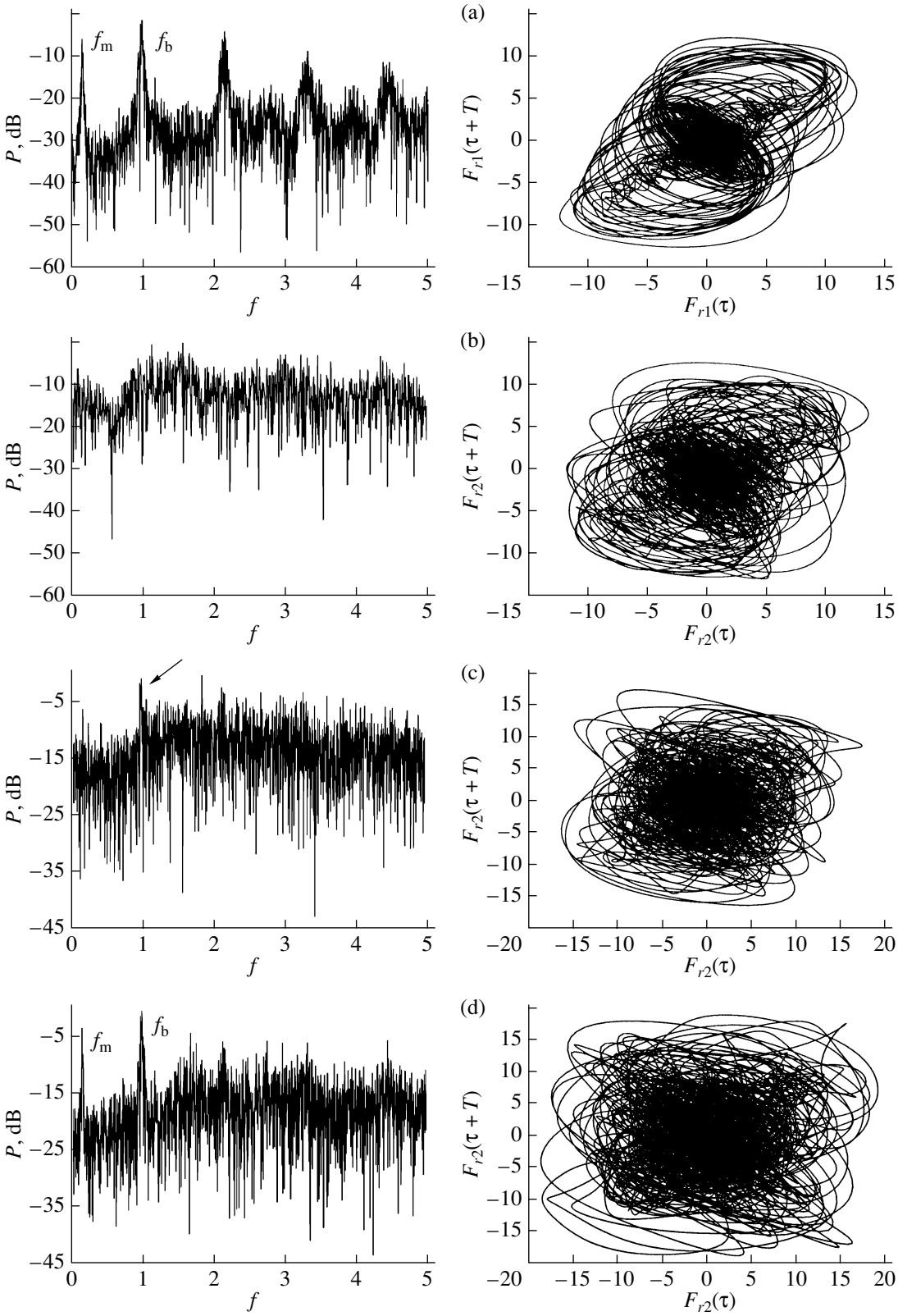


**Fig. 1.** Power spectra and phase portraits of oscillations in the independent (a) master and (b) slave BWOs and in the dependent slave system at $R$ = (c) 0.2 and (d) 0.5.

scale chaotic synchronization in the coupled active media is established.

Note that, as $R$ increases, time scales are first synchronized near basic scale $s_b$ (when $R = R_b$) (see Fig. 2) and then (for $R = R_m > R_b$) the phases of time scales lock in synchronism near basic scale $s_m$, which corresponds to the modulation frequency of the field at the BWO output.

Consider first the reason for the occurrence of range $\Delta s$ of synchronized scales (i.e., scales on which synchronism criteria (5) and (6) are fulfilled near basic frequency $f_b = 1/s_b$. To this end, let us turn to wavelet power spectra $\langle E_{1,2}(s)\rangle$, given by (4), for the master and slave media. The wavelet oscillation spectra of the output field for the master (dashed line *1*) and slave (continuous line *2*) BWOs are shown in Fig. 3 for various $R$. Wavelet spectrum $\langle E_1\rangle$ for the master BWO remains unchanged (for this medium, parameter $A_1$ is fixed and so the external field does not act on the medium) and is presented for comparison with wavelet power spectra $\langle E_2\rangle$ of the slave BWO.

Figure 3a demonstrates the wavelet oscillation power spectra for the self-excited oscillators. The wavelet spectra of the oscillators are seen to differ substantially. In wavelet spectrum $\langle E_1\rangle$ of the master system, basic time spectra $s_1$ (corresponding to high frequency $f_b$) and $s_m$ (modulated oscillations with fundamental frequency $f_m$) indicated in Fig. 3 stand out. In the wavelet spectrum of the slave system, the time scales corresponding to high-frequency spectral components (marked by an arrow in Fig. 3a) are distinctly seen, but the position of the peak in wavelet spectrum $\langle E_2\rangle$ does not correspond to basic time scale $s_b$ of the master subsystem. In other words, the basic frequencies of the subsystems diverge. For large scales (low modulation frequencies), the wavelet spectra are radically different. In the slave subsystem near scale $s_m$, the spectrum is continuous and uniform; that is, the modulated oscillations exhibit a continuous noise-like spectrum without peaks (time scales) on the background pedestal.

As $R$ increases, only those time scales meet synchronism conditions (5) and (6) for which the oscillation energy in the wavelet spectra of both subsystems is significant. In fact, at $R \approx 0.3$, the synchronism condition is met only for time scales near basic scale $s_b = 1/f_b \approx 1.0$ (see also Fig. 2). As follows from Fig. 3b, it is in this range of time scales that the wavelet oscillation energy is maximal.[1] From Fig. 3b, it is seen that the wavelet spectrum energy falling into scale $s_m$ of the master subsystem also grows. However, at $R \approx 0.3$, this

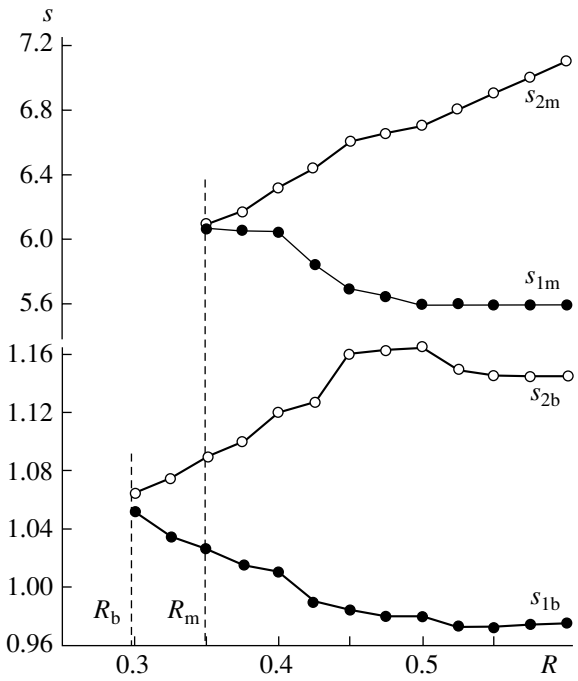


**Fig. 2.** Boundaries $s_1$ and $s_2$ of the synchronized time scale ranges on plane ($R$, $s$) for basic scales $s_b$ (lower curves) and $s_m$ (upper curves).

energy is small and the time scales of the field modulated oscillations are out of synchronism.

At high $R > 0.35$, the wavelet spectra of field oscillations at the outputs of both subsystems become similar to each other (Fig. 3c). The time scales corresponding to basic frequencies, $s_m$ and $s_b$, have roughly equal intensities. In this case, synchronization conditions (5) and (6) are met for the most intense (in terms of spectrum energy) time scales in the power spectra and, accordingly, two scale ranges where the phase lock in synchronism appear (Fig. 2, $R > 0.35$).

Thus, those time scales of field chaotic oscillations in the coupled active media are synchronized in the first place on which the energy of the oscillation power spectrum is significant.

With rising coupling coefficient, the range of the time scales for which conditions (5) and (6) are met expands. The scales adjacent to the most intense ones and also providing an appreciable spectrum energy become involved in the synchronous dynamics.

This is illustrated in Fig. 2, from which it is seen that, for both basic scales $s_b$ and $s_m$, range $\Delta s$ of scales being synchronized expands with increasing $R$. At a high coefficient of coupling between the BWOs, range $\Delta s_b = s_{2b} - s_{1b}$ of synchronized scales near basic scale $s_b$ stops expanding; moreover, it even contracts at $R > 0.5$. At the same time, near scale $s_m$, which describes the output field modulated, range $\Delta s_m = s_{2m} - s_{1m}$ of synchronized scales continues linearly expanding with $R$

[1] This range is shown by the hatched square and marked by letter *S* on the scale axis in Fig. 3.

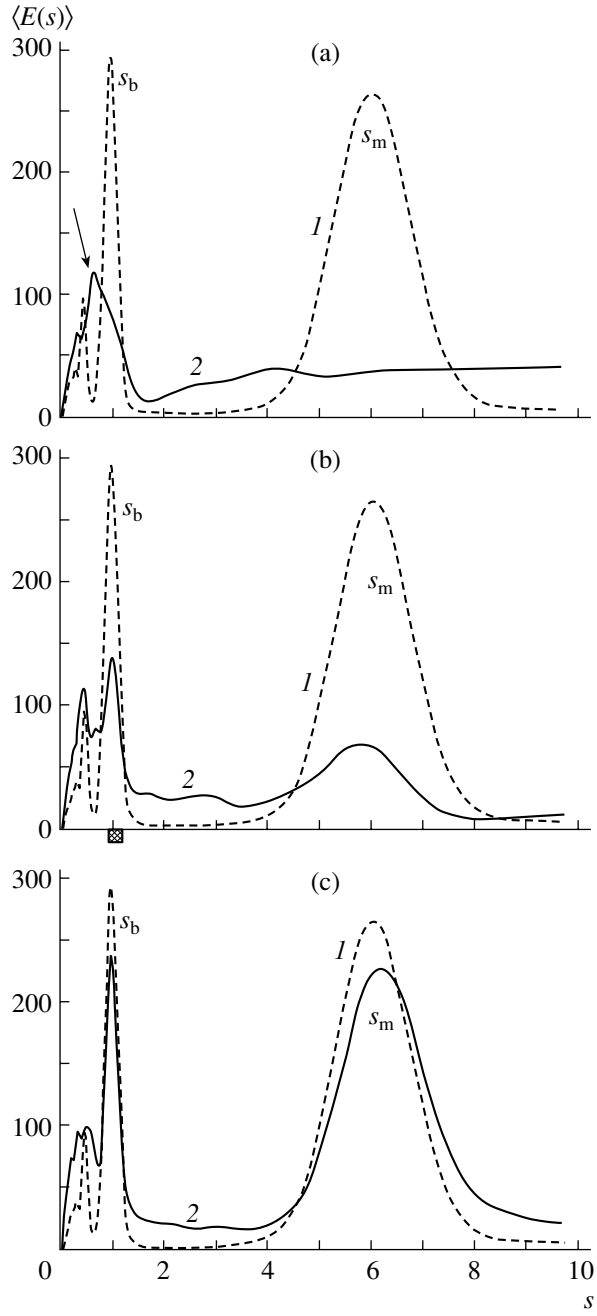


**Fig. 3.** Wavelet oscillation power spectra for the output field of the master (dashed curve *1*) and slave (continuous curve *2*) BWOs at $R$ = (a) 0, (b) 0.2, and (c) 0.5.

owing to the shift of the upper bound, $s_{2m}$, of this range. This is associated with the fact that, as $R$ increases, the energy in the wavelet spectrum of the slave subsystem is redistributed in such a way that larger scales ($s > s_m$) become more intense. Accordingly, the most intense time scales turn out to be brought to upper boundary $s_{2m}$ of the range of synchronism and it is these scales that are synchronized first with increasing $R$.

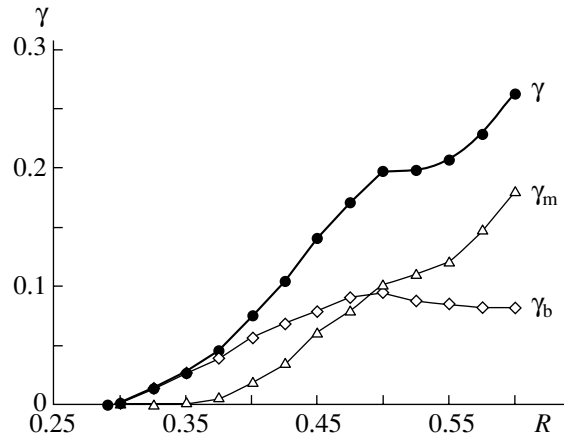


**Fig. 4.** $\gamma_b$, $\gamma_m$, and $\gamma$ vs. coupling $R$ between unidirectionally coupled BWOs.

## 3. MEASURE OF CHAOTIC SYNCHRONIZATION OF COUPLED ACTIVE ELECTRON-WAVE MEDIA

Introducing the continuous set of time scales $s$ and their associated chaotic signal phases, along with separating range $\Delta s = s_2 - s_1$ of scales synchronized, allows us to consider a quantitative measure of chaotic synchronization of coupled systems. It is defined as the fraction of the wavelet spectrum energy that is due to time scales synchronized [14],

$$\gamma = \int_{s_1}^{s_2} \langle E(s)\rangle ds \Big/ \int_0^\infty \langle E(s)\rangle ds, \qquad (14)$$

where $\langle E(s)\rangle$ is the integral distribution of the wavelet spectrum energy over scales (formula (4)).

If $\gamma = 0$, chaotic synchronization of coupled systems is absent. A nonzero value of $\gamma$ indicates the presence of synchronization, i.e., the presence of scales for which conditions (5) and (6) are valid. Finally, if $\gamma = 1$, oscillations in the systems are identical or are shifted relative to each other by some time interval $T_\tau$. The latter regime is referred to as the chaotic lag synchronization [2]. The growth of $\gamma$ from 0 to 1 means the increase in the energy due to time scales of synchronism. In essence, the value of $\gamma$ shows how much chaotic oscillations in coupled active media are close to each other.

In our case, when synchronism is observed for two basic scales, it is appropriate to introduce measures of synchronization $\gamma_b$ and $\gamma_m$ for each of scales $s_b$ and $s_m$, as well as the integral measure of synchronization, $\gamma = \gamma_b + \gamma_m$, of active distributed systems. The dependence of $\gamma$ on coupling coefficient $R$ characterizes the degree of chaotic synchronization of oscillations in coupled backward-wave electron-wave media.

Figure 4 demonstrates $\gamma_b$, $\gamma_m$, and $\gamma$ versus coefficient $R$ of coupling between the subsystems. For $R <$ 0.4–0.5, a major part of the oscillation energy due to

scales of synchronism falls on basic scale $s_b$ ($\gamma_b > \gamma_m$). In other words, frequencies $f \sim f_b$ (i.e., those that are close to the frequency of synchronism between the electron and electromagnetic waves in the active media) lock in synchronism first. Then, as $R$ grows, frequencies that are close to modulation frequency $f_m$ of the master BWO field lock in synchronism. With $R$ increasing further, more and more scales related to the low-frequency chaotic modulation of the BWO output signal become synchronized. Consequently, fraction $\gamma_m$ of the synchronized modulated low-frequency oscillation energy grows with $R$. At $R > 0.5$, the relative energy of synchronized modulated low-frequency oscillations, $\gamma_m$, exceeds $\gamma_b$, which characterizes the relative energy of synchronized high-frequency oscillations.

The integral fraction of the energy due to time scales of synchronism, $\gamma$, grows with the coupling factor amplitude, as follows from Fig. 4. However, even at high $R$, when the slave system is subjected to a rather intense signal ($R_2 = 0.3$–$0.4$) from the master, the fraction of the energy due to the scales synchronized does not exceed $\gamma \sim 0.3$.

Thus, when two unidirectionally coupled transverse-field BWOs are chaotically synchronized under the condition of increasing coupling coefficient, those time scales of oscillation are synchronized first that are close to time scale $s_b$, which is the most intense in the wavelet power spectrum and is close to the frequency of synchronism between the electron and electromagnetic waves. As $R$ grows, so does the energy due to synchronized scales near basic scale $s_b$. Simultaneously, time scale ranges $\Delta s_m$ that describe the low-frequency modulated oscillations of field $F$ in the BWOs lock in synchronism. With the coupling factor increasing further, the oscillation energy due to the time scales synchronized grows owing to the expansion of synchronized scale range $\Delta s_m$. Such behavior of two coupled BWOs is quantitatively described by the measure of mutual chaotic synchronization, $\gamma = \gamma(R)$.

## 4. SPATIAL DYNAMICS OF A SLAVE ACTIVE ELECTRON-WAVE MEDIUM

Consider now physical processes taking place when the chaotic synchronization conditions set up in a slave active medium with interacting counterpropagating waves. Emphasis will be on the spatial dynamics of the slave medium during the establishment of chaotic synchronization.

External chaotic signal $F_{ext1}(\tau) = F_1(\tau, \xi = 0)$ generated by the master (first) BWO strikes the slave BWO at point $\xi = L$ and then propagates toward the electron wave, i.e., toward the output, $\xi = 0$. Here, $L$ is the dimensionless length of the active medium ($L = 1.0$ in our normalization). Synchronization in the entire electron-wave system of the two media (i.e., the conditions studied above) means that the time scales of external signal $F_{ext1}(\tau)$ are synchronized with those of signal $F_{out2}(\tau) = F_2(\tau, \xi = 0)$ picked up from the output of the slave (second) medium. We will analyze the space–time dynamics of the slave in terms of synchronization of the time scales for external signal $F_{ext1}(\tau)$ and signals $F_2(\tau, \xi)$ picked up at different points of the slave system.

To be definite, consider the synchronization of time scales near scale $s_b$, which is the most intense in the wavelet power spectrum of the external chaotic signal. As was noted above, here time scale synchronization occurs at low $R$ (at low energies $P_{ext} = R^2|F_{ext1}|^2$ of the external signal). We will study range $\Delta s_b$ of time scales synchronized as a function of the spatial coordinate in the active medium. The dependence $\Delta s_b(\xi)$ and the measure of synchronization $\gamma(\xi)$ (see (14)) calculated from this dependence characterize the spatial dynamics of chaotic synchronization in an active medium subjected to an external chaotic signal at one of its ends.

Figure 5a shows the boundaries of the synchronized scale range in different sections of the space of interaction for three values of $R$. The curves are plotted on the coordinate plane [$s$, ($\xi - l$)], where $s$ is the time scale and ($\xi - L$) is the coordinate of the space of interaction that is measured from the entrance ($\xi = L$) to the system. The range where synchronization conditions (5) and (6) are met is the widest in the area adjacent to the boundary $\xi = L = 1.0$ to which the control signal from the master BWO is applied (see boundary conditions (13) for field $F_2$ of the slave BWO). With distance toward the exit from the BWO ($\xi = 0$), range $\Delta s_b$ of synchronized scales shrinks gradually. Measure of synchronization $\gamma_b(\xi)$ (Fig. 5b) varies over the space of interaction similarly to $\Delta s_b$. As coordinate $\xi$ of the space of interaction decreases, the wavelet oscillation spectrum energy due to synchronized scales decreases smoothly.

If $R$ is such that the chaotic synchronization of the coupled BWOs is absent ($R < 0.29$, see Sects. 2 and 3), the synchronized scale range goes down to zero over length of interaction $\xi_s$, $\xi_s < L$. In other words, the locking of phases corresponding to the time scales of variation of field $F_2(\tau, \xi)$, which occurs over the space of interaction in the dependent (slave) medium under the nonsynchronized chaotic conditions, has complex spatial dynamics. This dynamics is characterized by the following ranges of synchronized time scales:

$$\begin{aligned} \Delta s &\neq 0 \quad \text{for} \quad \xi > L - \xi, \\ \Delta s &= 0 \quad \text{for} \quad \xi < L - \xi_s. \end{aligned} \tag{15}$$

Then, we may argue that the slave active medium an be subdivided into two specific parts in the nonsynchronized regime. The first has length $\xi_s$ and occupies the interval ($L - \xi_s$, $L$), i.e., is adjacent to the entrance to the active medium ($\xi = L$). In this part, the oscillations of field $F_2(\tau, \xi)$ are chaotically synchronized with those of

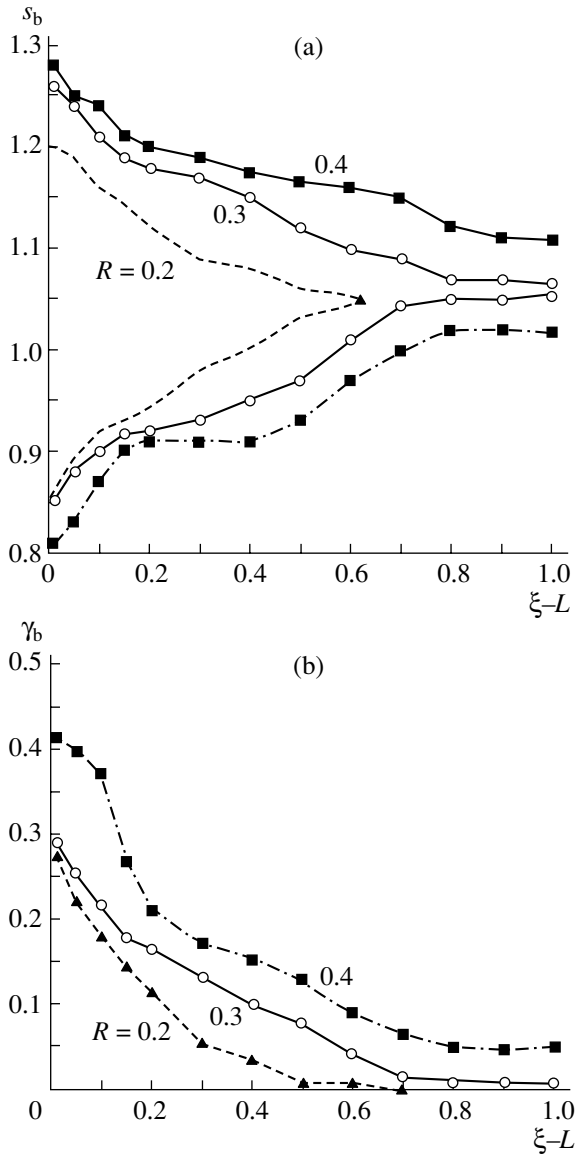


**Fig. 5.** (a) Boundaries of the synchronized time scale range on plane $[\gamma_b, (\xi - L)]$ (see text) and (b) measure of synchronization $\gamma_b(\xi)$ vs. coordinate $\xi - L$ in the space of interaction for various coupling factor amplitudes $R$.

input signal $F_{ext1}(\tau)$ (hence, the measure of chaotic synchronization is other than zero, $\gamma_b|_{\xi > L - \xi_s} \neq 0$) on time scales in some range $\Delta s$. This part is natural to call the region of synchronous oscillations; its length $\xi_s$, the length of synchronization. The other part, $\xi \in (0, L - \xi_s)$, is the region where chaotic synchronization breaks and where, accordingly, the range of synchronized time scales given by (15) and, hence, degree of synchronization $\gamma_b$ vanish.

Length of synchronization $\xi_s$ grows with the coupling coefficient and eventually becomes equal to the length of space of interaction, $\xi_s \equiv L$, at some $R = R_b$ (Fig. 2). This means that the chaotic synchronization conditions set up throughout the active electron-wave medium; that is, we may speak of the chaotic synchronization of the BWO as a whole. It is such conditions that were studied in the previous sections where the dynamics of time scales and their associated output ($\xi = 0$) chaotic signal of the slave was concerned.

The case of chaotic synchronization throughout the active medium is illustrated in Fig. 5a for $R = 0.3 \approx R_b$. Here, range $\Delta s$ of synchronized time scales is nonzero in all the sections of the medium; i.e., the process of chaotic synchronization covers the medium as a whole. As the coupling factor grows, range $\Delta s(\xi)$ of synchronized scales expands (Fig. 5a, $R = 0.4$), which is consistent with the previous results. In this case, the relative energy of the wavelet oscillation spectrum that falls on the synchronized time scales near the entrance ($\xi = L$) amounts to 30–40% at $\xi = 0.99L$. As the signal propagates over the space, $\gamma_b$ decreases, reaching 1–5% at the exit ($\xi = 0$).

It should be noted that similar results were obtained in our earlier work [9] for another distributed system subjected to a harmonic action. It was shown that an external harmonic signal interacting with chaotic oscillation in a traveling-wave gyrotron may establish both synchronization and asynchronous conditions, depending on its parameters. In the former case, the basic (most intense) spectral component in the power chaotic spectrum is locked in. In [9], the locking of the basic oscillation frequency was observed (as in this work) only over length $\Delta\xi < L$ in the space of interaction ($L$ is the length of the space of interaction in the gyrotron). The external harmonic action considered in [9] made it possible to analyze the locking of the single basic frequency in the chaotic oscillation spectrum but did not allow us to carefully study the process of establishing induced chaotic synchronization over the active medium.

Note in conclusion that the dependences shown in Fig. 5 are plotted on basic scale $s_b$. Similar dependences were obtained when the dynamics of synchronized scales near modulation scale $s_m$ was analyzed. The only difference is that, for $s_m$, the length of synchronization becomes equal to the length of the active medium at coupling factor amplitudes higher than for $s_b$, which is consistent with the results reported in the previous sections of this work.

## CONCLUSIONS

In this work, we used the new method [14] of analyzing chaotic synchronization that is based on introducing a set of time scales and their associated phases of a chaotic signal. The application of such an approach (instead of the conventional methods dealing with the chaotic signal phase) to chaotic oscillations in two unidirectionally coupled transverse-field BWOs allowed us to study chaotic synchronization in coupled elec-

tron-wave oscillators with complex dynamics (the conventional methods fail in studying chaotic signals with a complex topology of the attractor). In addition, the approach suggested made it possible to separate out the chaotic synchronization of low-frequency modulated oscillations of the field amplitude and the synchronization of high-frequency spectral components in the BWO oscillation spectrum. This would also have been impossible with the conventional methods of chaotic synchronization analysis.

It was shown that chaotic synchronization occurs with increasing coupling between microwave oscillators and shows up in a phase relation between the time scales of field chaotic oscillations in the master and slave systems. As the coupling factor grows, the phases of the power spectrum high-frequency components lock in synchronism first (there phases correspond to the synchronism frequencies of the electron and electromagnetic waves). The synchronization of the low-frequency modulated oscillations is observed at higher values of he coupling factor. In the asynchronous regime of chaotic oscillations, the space of the active medium can be subdivided into two regions. In one adjacent to the entrance to the system ($\xi = L$), the chaotic synchronization of the field oscillation time scales sets up. Synchronization length (the length of synchronous oscillation region) $\xi_s$ grows with coupling coefficient. The chaotic synchronization regime throughout the space of two coupled oscillators is established when the synchronization length of the slave becomes equal to the length of the active medium, $\xi_s = L$.

## ACKNOWLEDGMENTS

The authors thank D.I. Trubetskov for valuable discussions and comments.

This work was supported by the CRDF (grant no. REC-006), the program “Universities of Russia” (grant no. UR.01.01.051), the Federal Research Program “Dynasty,” and the International Center of Fundamental Physics.

## REFERENCES

1. M. G. Rosenblum, A. S. Pikovsky, and J. Kurths, Phys. Rev. Lett. **78**, 1804 (1996).
2. A. Pikovsky, M. Rosenblum, and J. Kurths, *Synchronization: Universal Concept in Nonlinear Sciences* (Cambridge Univ. Press, Cambridge, 2001).
3. C. M. Ticos, E. Rosa, W. B. Pardo, *et al.*, Phys. Rev. Lett. **85**, 2929 (2000).
4. V. A. Anishenko, A. G. Balanov, N. B. Janson, *et al.*, Int. J. Bifurcation Chaos Appl. Sci. Eng. **10**, 2339 (2000).
5. P. A. Tass, *et al.*, Phys. Rev. Lett. **90**, 088101 (2003).
6. M. D. Prokhorov, *et al.*, Phys. Rev. E **68**, 041913 (2003).
7. A. S. Dmitriev and A. I. Panas, *Dynamic Chaos: Advanced Data Carries for Communications* (Fizmatlit, Moscow, 2002) [in Russian].
8. A. A. Koronovskii, D. I.Trubetskov, and A. E. Hramov, Izv. Vyssh. Uchebn. Zaved. Radiofiz. **45**, 773 (2002).
9. D. I. Trubetskov and A. E. Hramov, Radiotekh. Élektron. (Moscow) **48**, 116 (2003).
10. N. M. Ryskin and V. N. Titov, Zh. Tekh. Fiz. **73** (9), 90 (2003) [ Tech. Phys. **48**, 1170 (2003)].
11. V. S. Anishenko and T. E. Vadivasova, Radiotekh. Élektron. (Moscow) **47**, 133 (2002).
12. A. Pikovsky, M. Rosenblum, and J. Kurths, Int. J. Bifurcation Chaos Appl. Sci. Eng. **10**, 2291 (2000).
13. V. S. Anishenko and T. E. Vadivasova, Radiotekh. Élektron. (Moscow) **49**, 123 (2004).
14. A. A. Koronovskii and A. E. Hramov, Pis’ma Zh. Éksp. Teor. Fiz. **79**, 391 (2004) [JETP Lett. **79**, 316 (2004)].
15. *Wavelets in Physics*, Ed. by J. C. van den Berg (Cambridge Univ. Press, Cambridge, 1998).
16. A. A. Koronovskii and A. E. Hramov, *Continuous Wavelet Analysis and Its Applications* (Fizmatlit, Moscow, 2003) [in Russian].
17. D. I. Trubetskov and A. E. Hramov, *Lectures on Microwave Electronics for Physicists* (Fizmatlit, Moscow, 2003), Vol. 1 [in Russian].
18. A. P. Chetverikov Izv. Akad. Nauk, Ser. Fiz. **58**, 171 (1994).
19. A. V. Gaponov, M. I. Petelin, and V. K. Yulpatov, Izv. Vyssh. Uchebn. Zaved. Radiofiz. **10**, 1415 (1967).
20. S. P. Kuznetsov and A. P. Chetverikov, Izv. Vyssh. Uchebn. Zaved. Radiofiz. **24**, 109 (1981).
21. A. P. Chetverikov, Vyssh. Uchebn. Zaved. Prikl. Nelin. Din. **2** (5), 46 (1994).
22. J. Kurths and A. S. Pikovsky, Chaos, Solitons and Fractals **5**, 1893 (1995).
23. F. Takens, *Lectures Notes in Mathematics*, Ed. by D. Rand and L.-S. Young (Springer Verlag, New York, 1981).
24. A. A. Koronovskii, D. I.Trubetskov, and A. E. Hramov, Dokl. Akad. Nauk **395**, 143 (2004) [Dokl. Phys. **49** , 143 (2004)].

*Translated by V. Isaakyan*